

# Superdirective Beamforming Using an Extended Modal Subspace Decomposition

Martin Eichler and Arild Lacroix

*J. W. Goethe Universität, Institut für Angewandte Physik, 60438 Frankfurt am Main*

*Email: {Eichler, Lacroix}@iap.uni-frankfurt.de*

## Introduction

Beamforming techniques allow to control the characteristic of a microphone array in order to achieve a desired directivity. One of the most general formulations is the filter-and-sum beamformer which has readily been generalized by the concept of Modal Subspace Decomposition. This approach finds optimum FIR filter coefficients for each sensor by solving an eigenvalue problem and projecting the desired beam pattern to the set of eigen-beam patterns found. However, the resulting beamformers fail to be directive at very low frequencies. In this contribution, we propose an extension to the mentioned concept of Modal Subspace Decomposition, which helps to overcome this problem by making the algorithm approximately superdirective.

## Beamforming

We consider a sound field built up by planar waves having the wave vectors  $\underline{k} \in K$ , with  $K \subset \mathfrak{K}$  being the considered *finite* range from the wave number vector space  $\mathfrak{K}$ . Given a source amplitude distribution  $S(\underline{k})$ , the sound pressure at the location  $\underline{r}$  and time  $t$  takes the form

$$p(\underline{r}, t) = \iint_K S(\underline{k}) \cdot e^{i(\omega(\underline{k})t - \underline{k} \cdot \underline{r})} d^2k,$$

where  $\omega(\underline{k}) = kc$  with  $k := \|\underline{k}\|$  and  $c$  is the sound velocity. The output signal  $y(t)$  of a filter-and-sum beamformer having  $N$  sensors at the positions  $\underline{r}_n$  can then be written as

$$\begin{aligned} y(t) &= \iint_K \sum_{n=0}^{N-1} S(\underline{k}) \cdot H_n(\omega(\underline{k})) \cdot e^{i(\omega(\underline{k})t - \underline{k} \cdot \underline{r}_n)} d^2k \\ &= \iint_K S(\underline{k}) \cdot B(\underline{k}) \cdot e^{i\omega(\underline{k})t} d^2k, \end{aligned}$$

where the  $H_n(\omega)$  are the transfer functions of the weighting filters for each sensor and

$$B(\underline{k}) = \sum_{n=0}^{N-1} H_n(\omega = kc) \cdot e^{-i\underline{k} \cdot \underline{r}_n} \quad (1)$$

is the so-called *beam pattern* describing the beamformer sensitivity as a function of angle and frequency. First, we consider two spatial dimensions; the extension to three dimensions can be done by changing all double integrals to triple ones. Let us assume weighting filters of the form

$$H_n(\omega) = \sum_{l=0}^{L-1} h_{n,l} \cdot e^{-i\omega \Delta t_{n,l}} \quad \text{for } n = 0 \dots N-1, \quad (2)$$

where  $\Delta t_{n,l}$  are arbitrary time delays ( $\Delta t_{n,l} \neq \Delta t_{n,l'}$  for  $l \neq l'$ ). If  $\Delta t_{n,l}$  are multiples of a constant  $T_S$ :  $\Delta t_{n,l} = l \cdot T_S$ , then the  $H_n$  are digital FIR filters of  $(L-1)$ th order, operating at a samplerate of  $f_S = 1/T_S$ . Substituting (2) into (1), we see that the beam pattern comprises  $V = NL$  summands, which can be expressed as

$$B(\underline{k}) = \sum_{\nu=0}^{V-1} \tilde{H}_\nu(kc) \cdot e^{-i\underline{k} \cdot \underline{r}_\nu}, \quad (3)$$

using the definitions ( $\nu = nL + l$ )

$$\begin{aligned} \tilde{H}_{\nu=nL+l}(\omega) &= w_{nL+l} \cdot e^{-i\omega \Delta t_{n,l}} \\ w_{\nu=nL+l} &= h_{n,l} \\ \underline{r}_{\nu=nL+l} &= \underline{r}_n \end{aligned} \quad (4)$$

with  $n = 0 \dots N-1$  and  $l = 0 \dots L-1$ . If we further define the *unit delay filter*  $D(\omega) = e^{-i\omega T_S}$  and the dimensionless delay  $\tau_{\nu=nL+l} = \Delta t_{n,l}/T_S$ , we can rewrite (4) as

$$\tilde{H}_\nu(\omega) = w_\nu \cdot (D(\omega))^{\tau_\nu}. \quad (5)$$

We thus have  $L$  delay filters ( $\tilde{H}_{nL} \dots \tilde{H}_{nL+(L-1)}$ ) acting on the signal from the  $n$ th sensor, each with an individual delay  $\tau_\nu$ . Using this formulation and further defining

$$\hat{A}(\underline{k}) = (D(kc)^{\tau_0} \cdot e^{-i\underline{k} \cdot \underline{r}_0}, \dots, D(kc)^{\tau_{V-1}} \cdot e^{-i\underline{k} \cdot \underline{r}_{V-1}}) \quad (6)$$

along with a coefficient vector  $\underline{w} = (w_0, \dots, w_{V-1})^T$  (where the superscript  $T$  denotes the transpose), the beam pattern (3) finally takes the form

$$B(\underline{k}) = \sum_{\nu=0}^{V-1} A_\nu(\underline{k}) \cdot w_\nu = \hat{A} \underline{w}. \quad (7)$$

The *operator*  $\hat{A}$  is dependent on the wave vector  $\underline{k}$ ; the coefficient vector  $\underline{w}$  controls the overall beam pattern.

## Modal Subspace Decomposition

A big variety of methods exists to obtain suitable filter coefficients for a given beamforming task [1]. One approach treats this task as an *eigenvalue problem*: We consider the  $V$ -dimensional complex vector space  $\mathfrak{V} = \mathbb{C}^V$  and assume a coefficient vector  $\underline{w} \in \mathfrak{V}$ .  $\hat{A}$  is a linear map  $\hat{A} : \mathfrak{V} \rightarrow \mathfrak{F}$ , where  $\mathfrak{F}$  is the function space of all *achievable* beam patterns:  $\mathfrak{F} = \{B(\underline{k}) | B = \hat{A} \underline{w} \wedge \underline{w} \in \mathfrak{V}\}$ , and each vector  $\underline{w} \in \mathfrak{V}$  is mapped to a beam pattern  $B$ :  $\hat{A} : \underline{w} \mapsto B(\underline{k}) = \hat{A} \underline{w}$ . Now we define the inner products

$$\langle \underline{w} | \underline{w}' \rangle_{\mathfrak{V}} = \sum_{\nu=0}^{V-1} w_\nu \cdot w'_\nu, \quad (8)$$

$$\langle B(\underline{k}) | B'(\underline{k}) \rangle_{\mathfrak{F}} = \iint_K B(\underline{k}) \cdot B'^*(\underline{k}) d^2k \quad (9)$$

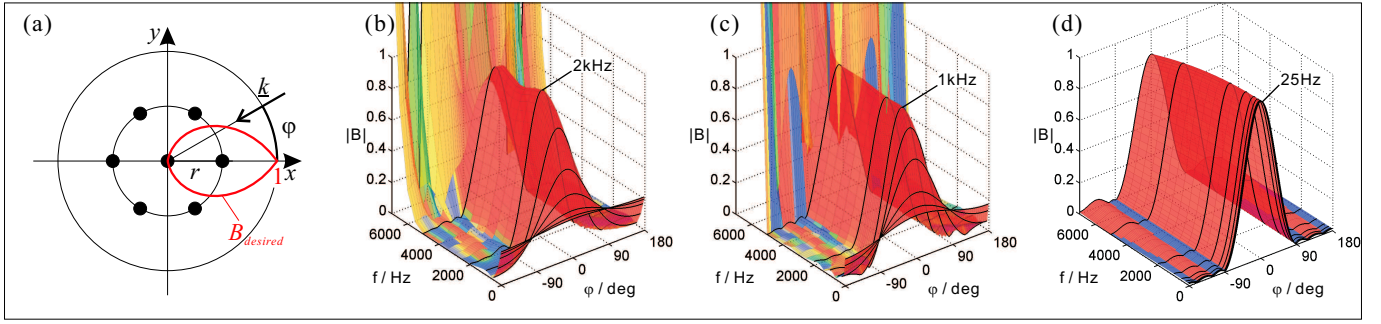


**Figure 1:** Beamforming example, two-dimensional case (2-D). (a) Sensor locations (black dots,  $r = 1$  cm) and desired beam pattern (red); (b) MSD beamformer, design frequency range 25 Hz–5 kHz, 3rd order ( $L = 3$ ); (c) same as (b), but 10th order ( $L = 10$ ); (d) SMB beamformer. The black curves outline the beam patterns at 25, 50, 100, 250, 500, 1000, 2000, 5000 and 7000 Hz. Color indicates the phase (c.f. fig. 3).

for  $\underline{w}, \underline{w}' \in \mathfrak{V}$  and  $B, B' \in \mathfrak{F}$ , with  $*$  denoting the complex conjugate. It is possible to find an *adjoint operator*  $\hat{A}^\dagger : \mathfrak{F} \rightarrow \mathfrak{V}$  mapping a beam pattern  $B$  to a vector  $\underline{w} = \hat{A}^\dagger B$  having the property  $\langle \hat{A}^\dagger B | \underline{w}' \rangle_{\mathfrak{V}} = \langle B | \hat{A} \underline{w}' \rangle_{\mathfrak{F}}$  for  $B \in \mathfrak{F}$  and  $\underline{w}' \in \mathfrak{V}$  [2]: Using (8) and (9), we write

$$\begin{aligned} \langle B | \hat{A} \underline{w}' \rangle_{\mathfrak{F}} &= \iint_K B(\underline{k}) \cdot \sum_{\nu=0}^{V-1} A_\nu^* \cdot w'_\nu \cdot d^2k \\ &= \sum_{\nu=0}^{V-1} w'_\nu \cdot \underbrace{\left[ \iint_K A_\nu^* \cdot B(\underline{k}) \cdot d^2k \right]}_{(\hat{A}^\dagger B(\underline{k}))_\nu} \\ &\stackrel{!}{=} \langle \hat{A}^\dagger B | \underline{w}' \rangle_{\mathfrak{V}} = \sum_{\nu=0}^{V-1} (\hat{A}^\dagger B(\underline{k}))_\nu \cdot w'_\nu \cdot \end{aligned}$$

Comparing the last two lines, the elements of the adjoint operator  $\hat{A}^\dagger$  can be identified, which thus takes the form

$$\hat{A}^\dagger = \begin{pmatrix} \iint_K d^2k A_0^* \cdot \square \\ \vdots \\ \iint_K d^2k A_{V-1}^* \cdot \square \end{pmatrix}, \quad (10)$$

where the boxes  $\square$  indicate that the integrands of  $\iint_K d^2k$  must contain the respective operand which is multiplied from the right side. Now we consider the matrix  $\mathbf{Z} = \hat{A}^\dagger \hat{A}$ . With  $\hat{A} = (A_0, \dots, A_{V-1})$ , it follows from (10) that the matrix elements of  $\mathbf{Z}$  take the form ( $\nu, \nu' = 0 \dots V-1$ )

$$Z_{\nu\nu'} = \iint_K A_\nu^* \cdot A_{\nu'} \cdot d^2k. \quad (11)$$

The integral in (11) is carried out over all angles, restricting  $k = \|\underline{k}\|$  to a finite interval  $k \in [k_1; k_2]$ . Through  $k_{1,2} = 2\pi f_{1,2}/c$ , this corresponds to a frequency range  $[f_1; f_2]$  which will be referred to as *design frequency range*. Now, by finding the  $V$  normalized eigenvectors  $\underline{u}_\nu$  and eigenvalues  $\lambda_\nu$  of  $\mathbf{Z}$  (which is a  $V \times V$  matrix), a complete orthonormal basis of the vectorspace  $\mathfrak{V}$  is obtained. This basis corresponds to a set of  $V$  orthonormalized functions  $U_\nu(\underline{k}) = \hat{A} \underline{u}_\nu / \sqrt{\lambda_\nu}$  which are eigenfunctions of  $\hat{A} \hat{A}^\dagger$  with the same eigenvalues and form a complete orthonormal basis of  $\mathfrak{F}$ , such that

$$\langle \underline{u}_\nu | \underline{u}_{\nu'} \rangle_{\mathfrak{V}} = \delta_{\nu\nu'} \quad \text{and} \quad \langle U_\nu | U_{\nu'} \rangle_{\mathfrak{F}} = \delta_{\nu\nu'}$$

holds,  $\delta$  denoting the Kronecker delta. A given desired beam pattern can now be projected to  $\mathfrak{F}$  (which is a *subspace* of the space of *all* possible beam patterns) and be approximated by a linear combination of the  $U_\nu(\underline{k})$ :

$$\begin{aligned} B_{approx}(\underline{k}) &= \hat{A} \underline{b} \quad (12) \\ \underline{b} &= \sum_{\nu=0}^{V-1} \frac{1}{\sqrt{\lambda_\nu}} \cdot \langle B_{desired}(\underline{k}) | U_\nu(\underline{k}) \rangle_{\mathfrak{F}} \cdot \underline{u}_\nu. \quad (13) \end{aligned}$$

This is an approximation because the desired beam pattern may lie outside  $\mathfrak{F}$ . Yet, the approximation is optimal in the sense that the mean-squared error is minimized. This approach is called *Modal Subspace Decomposition* (MSD) and is discussed in more detail in [2].

## Superdirective Extension

We will now discuss a modification of the above MSD approach, leading to superdirectivity. It is motivated by two observations: Firstly, MSD fails to achieve directivity at very low frequencies (see example in fig. 1(a)–(c), more detailed discussion in the „Examples“ section). Secondly, differential arrays can be used to build *Superdirective Multipole Beamformers* (SMB) where superdirectivity of a multipole of order  $\mu$  is obtained by  $\mu$ -fold integration over time (fig. 1(d); detailed discussion in [3] and [4]). We hence consider  $L$  integration filters for each one of the  $N$  sensors, performing a  $0 \dots L-1$ -fold integration over time on the respective signal (see diagram in fig. 2). This gives a total of  $V = NL$  filters defined as

$$\tilde{H}_\nu(\omega = kc) = w_\nu \cdot \left( \frac{a}{ik} \right)^{\mu\nu} = w_\nu \cdot (G(\omega))^{\mu\nu}, \quad (14)$$

where  $G(\omega) = ac/i\omega$  is a single integrating filter and  $\mu_\nu$  is the *integration order* defined as  $\mu_{\nu=nL+l} = l$  (with  $n = 0 \dots N-1, l = 0 \dots L-1$  and  $\nu = nL+l = 0 \dots V-1$ ). The factor  $a$  (unit:  $\text{m}^{-1}$ ) is introduced to make the terms  $ac/i\omega$  and  $a/ik$  dimensionless, and will be discussed later. To obtain an operator representation of the new beamformer, we compare (14) to (5) and adapt (6) by replacing  $D$  by  $G$  and  $\tau$  by  $\mu$ . We get

$$\hat{A}(\underline{k}) = \left( \left( \frac{a}{ik} \right)^{\mu_0} \cdot e^{-ik \cdot \tilde{r}_0}, \dots, \left( \frac{a}{ik} \right)^{\mu_{V-1}} \cdot e^{-ik \cdot \tilde{r}_{V-1}} \right). \quad (15)$$

By substituting the elements of (15) into (10) and (11), the adjoint operator  $\hat{A}^\dagger$  and the matrix elements of  $\mathbf{Z}$  are

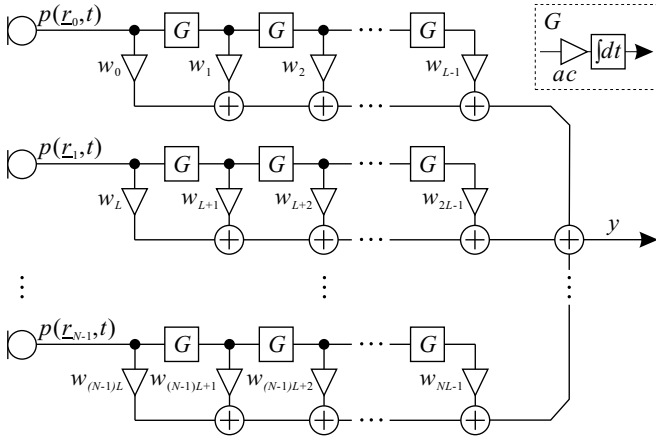


**Figure 2:** Signal flow diagram of the proposed beamformer. Each of the  $N$  sensor signals is integrated 0 to  $L-1$  times by means of the filters  $G(\omega) = ac/i\omega$ .

obtained. The latter take the form ( $\nu, \nu' = 0 \dots V-1$ )

$$Z_{\nu\nu'} = (-1)^{\mu\nu} \iint_K \left(\frac{a}{ik}\right)^{\mu\nu+\mu\nu'} \cdot e^{-ik \cdot (\tilde{r}_{\nu'} - \tilde{r}_{\nu})} d^2k. \quad (16)$$

It can be seen from (16) that  $\mathbf{Z}$  is Hermitian ( $Z_{lm} = Z_{ml}^*$ ). Thus, its eigenvalues are real and its eigenvectors are orthogonal and can, after normalization, be used as an orthonormal base  $\{\underline{u}_{\nu}\}$  of  $\mathfrak{B}$ . We now evaluate the matrix elements (16), restricting the regarded wave number range  $K$  to a bandlimited design range of frequencies, i.e.  $k_1 \leq k \leq k_2$ , but allowing *all* propagation directions.

### Two-Dimensional Case

For two dimensions (2-D), to so-defined  $K$  is a ring-shaped area around the origin in the  $x$ - $y$  plane of  $\mathfrak{R}$ . This requires the use of polar coordinates in the  $x$ - $y$  plane, e.g.

$$\underline{k} = -k \cdot \begin{pmatrix} \cos \varphi \\ \sin \varphi \end{pmatrix} \quad \text{and} \quad \tilde{r}_{\nu} = \begin{pmatrix} \tilde{x}_{\nu} \\ \tilde{y}_{\nu} \end{pmatrix},$$

with the volume element  $d^2k = k dk d\varphi$ . The integration over the angle ( $-\pi \leq \varphi \leq \pi$ ) can now be performed separately and only the integration over frequency remains, such that (16) reduces to

$$Z_{\nu\nu'}^{2D} = 2\pi(-1)^{\mu\nu} \int_{k_1}^{k_2} \left(\frac{a}{ik}\right)^{\mu\nu+\mu\nu'} J_0(k\|\tilde{r}_{\nu'} - \tilde{r}_{\nu}\|) k dk, \quad (17)$$

where  $J_0(x)$  is the 0<sup>th</sup>-order Bessel function of the first kind. After calculating  $\mathbf{Z}$  and identifying its eigenvalues  $\lambda_{\nu}$  and eigenvectors  $\underline{u}_{\nu}$ , it is now possible to approximate a given desired beam pattern using eqs. (12) and (13).

### Three-Dimensional Case

For three spatial dimensions (3-D),  $K$  forms a spherical shell around the origin of  $\mathfrak{R}$ . We hence use spherical coordinates, e.g.

$$\underline{k} = -k \cdot \begin{pmatrix} \cos \varphi \cdot \sin \theta \\ \sin \varphi \cdot \sin \theta \\ \cos \theta \end{pmatrix} \quad \text{and} \quad \tilde{r}_{\nu} = \begin{pmatrix} \tilde{x}_{\nu} \\ \tilde{y}_{\nu} \\ \tilde{z}_{\nu} \end{pmatrix},$$

with  $-\pi \leq \varphi \leq \pi$  and  $0 \leq \theta \leq \pi$ , the volume element being  $d^3k = k^2 \sin \theta dk d\varphi d\theta$ . Further, we need to extend

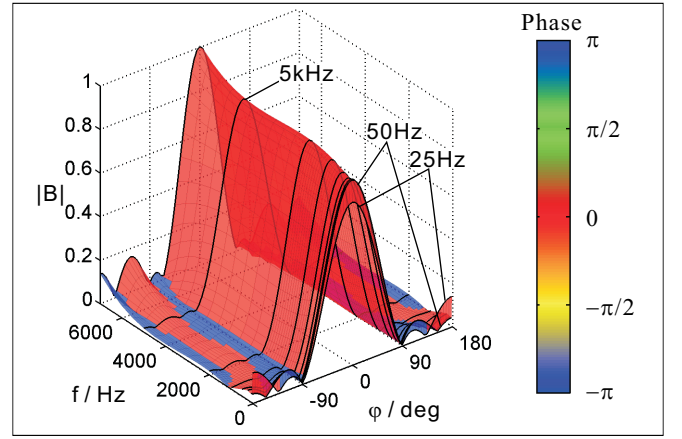


**Figure 3:** Beamforming example (2-D) as in fig. 1, but using the proposed superdirective extension. The phase of the complex-valued beam pattern  $B(\underline{k})$  is indicated by color.

the so-far presented theory to three dimensions, which luckily results in simply replacing all double integrals ( $\iint_K d^2k$ ) by triple ones ( $\iiint_K d^3k$ ). Importantly, the inner product (9) changes to

$$\langle B(\underline{k}) | B'(\underline{k}) \rangle_{\mathfrak{B}} = \iiint_K B(\underline{k}) \cdot B'^*(\underline{k}) d^3k. \quad (18)$$

Evaluating (16) in its modified triple-integral form, the integration over the angles  $\varphi$  and  $\theta$  can again be carried out independently, yielding

$$Z_{\nu\nu'}^{3D} = 4\pi(-1)^{\mu\nu} \int_{k_1}^{k_2} \left(\frac{a}{ik}\right)^{\mu\nu+\mu\nu'} \text{si}(k\|\tilde{r}_{\nu'} - \tilde{r}_{\nu}\|) k^2 dk, \quad (19)$$

where  $\text{si}(x) = \sin(x)/x$  is the unnormalized sinc function. Note that for the evaluation of (13), now the modified inner product (18) must be used.

Regarding the factor  $a$  introduced in (14), it shall be mentioned that its value does not affect the beamforming results. Though it obviously influences the matrix  $\mathbf{Z}$  along with its eigenvalues and eigenvectors, it can be shown analytically that the approximating beam pattern found using eqs. (12) and (13) is independent of  $a$ . Intuitively speaking, this is evident because the value of  $a$  solely distorts the relation between the coefficients  $w_{\nu}$  and the terms  $\tilde{H}_{\nu} \cdot e^{-ik \cdot \tilde{r}_{\nu}}$  which build up the beam pattern, while the *manifold of achievable beam patterns* is not altered. Thus, the optimum beam pattern must be the same, even if its generating coefficient vector, depending on  $a$ , may look different.  $a$  can therefore safely be set to  $1 \text{ m}^{-1}$  or even be ignored. Yet, its use lies in the fact that it makes the matrix  $\mathbf{Z}$  dimensionless, so we don't have to consider units in the eigenvectors and in the coefficient vector.

## Examples

We will now discuss some beamforming examples. For the two-dimensional case, we consider a seven-sensor array ( $N = 7$ ) and a desired beam pattern as depicted in fig. 1(a). As design range,  $[f_1; f_2] = [25 \text{ Hz}; 5 \text{ kHz}]$  is

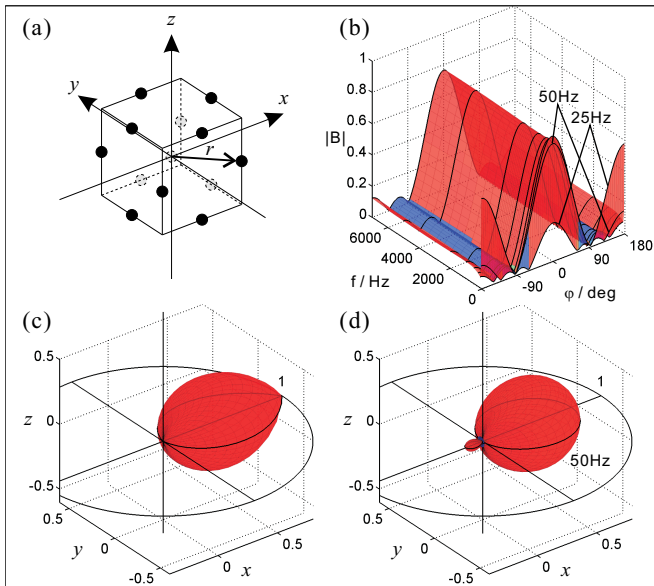


**Figure 4:** Beamforming (3-D) using the proposed superdirective extension. (a) Geometry: 12 sensors aligned at the middle of the edges of a cube centered at the origin, each at distance  $r = 1$  cm from the origin, one 13th sensor at the origin itself; (b) azimuth beam pattern; (c) desired beam pattern; (d) achieved spatial beam pattern at  $f = 50$  Hz.

chosen. Fig. 1(b) and 1(c) show the beamforming result using MSD (beamformer defined by eqs. (3), (5), (6), (7)), (b):  $L = 3$ ; (c):  $L = 10$  (for the matrix elements, see [2]). Fig. 1(d) shows the realization of the same desired beam pattern using the SMB method [3, 4]. In fig. 3, the result obtained by the above superdirective extension is depicted (beamformer defined by eqs. (3), (7), (14), (15); matrix elements according to (17)),  $L = 3$ . All integrals were approximated using the trapezoidal rule. It can be seen that MSD has almost no directivity at 25 Hz and only gradually approaches the desired beam pattern. For order  $L = 3$ , full directivity is reached at  $\approx 2$  kHz (fig. 1(b)), for  $L = 10$  at  $\approx 1$  kHz (fig. 1(c)). Further, the beam pattern diverges rapidly with increasing frequency outside the design range ( $f > 5$  kHz). This is caused by certain eigenfunctions which grow very large at high frequencies. In contrast, the SMB (fig. 1(d)) is directive at 25 Hz already (superdirectivity). This property – and a second effect of the integration filters – can be found in the results obtained by the superdirective extension (fig. 3): Directivity is achieved at much lower frequencies, and the divergence outside the design range ( $f > 5$  kHz) is much slower. However, the behaviour at the lower design frequency range boundary (25–50 Hz) is not exactly superdirective, as can be seen from the magnitude fluctuations. Yet, this problem can be avoided to some extent by lowering the lower design range boundary frequency such that the lowest frequency of interest lies well inside the design range. The same effect can also be observed in the three-dimensional example shown in fig. 4. Here, the superdirective extension is evaluated using the matrix elements (19) for the 13-sensor geometry depicted in fig. 4(a). The desired beam pattern (fig. 4(c)) is defined by rotating the one shown in fig. 1(a) around the  $x$  axis. Fig. 4(d) shows the three-dimensional beam

pattern at 50 Hz, while fig. 4(b) shows the beam pattern over frequency at  $\theta = 90^\circ$  along the azimuth angle  $\varphi$ . The desired beam pattern is matched very well from 50 Hz upwards, while at the border frequency 25 Hz, the result is very different to the desired one. (Further calculations show that this can be improved greatly by extending the design frequency range downward to 10 Hz.) It should be mentioned that numerical errors (e.g. in integral approximation or other) can cause some of the eigenfunctions of  $\hat{A}\hat{A}^\dagger$  corresponding to the smallest eigenvalues  $\lambda_\nu$  to be not orthonormalized. Such eigenfunctions can impair the beam pattern and should be excluded from the series expansion.

## Summary

In this paper, an extension to the known concept of *Modal Subspace Decomposition* MSD is presented which introduces several integration filters into the signal path of each sensor. The beamformer is represented by an operator  $\hat{A}$  mapping a coefficient vector  $\underline{w}$  to a beam pattern  $B(\underline{k}) = \hat{A}\underline{w}$ . The desired beam pattern is then approximated by a series expansion using the eigenfunctions of  $\hat{A}\hat{A}^\dagger$ . This approach combines interesting properties of both MSD and SMB: It achieves superdirective beam patterns (like multipoles), it is applicable to arbitrary sensor geometries (2-D/3-D), and it allows optimization for a given frequency range of interest. However, as is also the case for SMB, the maximum integration order  $L$  cannot be raised arbitrarily due to stability problems with manifold integration at frequencies near zero. One interesting further extension of the presented approach might be to replace each of the coefficients in  $\underline{w}$  by an FIR filter of length  $M$ . Pursuing the above strategy, one would obtain a similar operator notation with  $V' = M \cdot N \cdot L$  coefficients. This may imply a disadvantageous increase in numerical complexity. For frequency-selective beamforming, it is hence more reasonable to add an FIR or IIR filter to the beamformer output.

## References

- [1] M. Brandstein, D. Ward (eds.), “Microphone Arrays - Signal Processing Techniques and Applications”, Springer-Verlag, Berlin, Heidelberg, New York, 2001.
- [2] M. I. Y. Williams, T. D. Abhayapala, R. A. Kennedy, “Generalized Broadband Beamforming Using a Modal Subspace Decomposition”, *EURASIP Journal on Advances in Signal Processing*, vol. 2007, Article ID 68291, 9 pages, doi:10.1155/2007/68291, 2007.
- [3] M. Eichler, A. Lacroix, „Broadband Superdirective Beamforming Using Multipole Superposition“, in *Proc. EUSIPCO 2008*, CD-ROM, Lausanne, Swiss, Aug. 2008.
- [4] M. Eichler, A. Lacroix, „Spatial Filtering Using A Higher-Order Differential Microphone Array“, *ITG-Fachtagung Sprachkommunikation 2008*, VDE-Verlag, ITG-Fachbericht Band 211, CD-ROM, ISBN 978-3-8007-3120-6, Aachen, Germany, Oct. 2008.